Available online at www.sciencedirect.com
ScienceDirect
Ceramics International 35 (2009) 1587–1594
CERAMICS INTERNATIONAL
www.elsevier.com/locate/ceramint

Calcium phosphate granules for use as a 5-Fluorouracil delivery system

C. Santos [a], M.A. Martins [b], R.-P. Franke [c], M.M. Almeida [a], M.E.V. Costa [a,*]

[a] Department of Ceramic and Glass Engineering, CICECO, University of Aveiro, Campus Universitário de Santiago, 3810-193 Aveiro, Portugal
[b] Department of Chemistry, CICECO, University of Aveiro, 3810-193 Aveiro, Portugal
[c] Department of Biomaterials, University of Ulm, 89081 Ulm, Germany

Received 17 July 2008; received in revised form 2 August 2008; accepted 28 August 2008
Available online 30 September 2008

Abstract

The possibility of tailoring apatite granules as a controlled release system for the drug model 5-Fluorouracil (5FU) has been examined. Apatite granules (SDG) were obtained by spray drying suspensions of hydroxyapatite (HAP) nanoparticles previously precipitated from citrate solutions [M.A. Martins, C. Santos, M.E.V. Costa, M.M. Almeida, Preparation of porous hydroxyapatite particles to be used as drug delivery systems, Advanced Materials Forum II (455) (2004) 353–357]. SDG had donut shape and very high specific surface area (150 m^2/g) indicative of high porosity. SDG were poorly crystalline HAP but turned into biphasic granules (HSDG) with crystalline tricalcium phosphate and HAP after annealing at 800 °C, while reducing their surface area down to ~6 m^2/g. SDG and HSDG were soaked in a 5FU solution at pH 5.2 and room temperature during several days and then transferred to a phosphate buffered solution (PBS) at pH 7.4 and 37 °C, for releasing 5FU. The comparison between the 5FU adsorbing and releasing behaviours exhibited by SDG and HSDG shows that engineering the granules characteristics, i.e. specific surface area, surface chemical composition, porosity and crystal phase composition allows the 5FU release profile to be controlled.

Keywords: D. Apatite; E. Biomedical applications; Spray drying; 5-Fluorouracil

1. Introduction

Synthetic calcium phosphate (CaP) based materials such as hydroxyapatite (HAP) and β-tricalcium phosphate (β-TCP) are compounds with high potential for bioapplications [2–4]. HAP ($Ca_{10}(PO_4)_6(OH)_2$) exhibits excellent biocompability and bioactivity, possibly due to its compositional similarity to the mineral constituents of bone and teeth [5,6]. Besides its extensively studied application in the reconstruction of damaged tissue [7,8], its ability to adsorb substances of biological interest makes it an attractive material for drug delivery systems. Although stoichiometric HAP is the less soluble and more stable CaP material, its Ca deficient non-stoichiometric form is the most often synthesized one due to the possibility of multiple atomic substitutions in its structure.

β-TCP ($Ca_3(PO_4)_2$), another promising material for biomedical applications [9], is a slowly degrading bioresorbable calcium phosphate with a pure hexagonal crystal structure [10]. Its significant biological affinity and activity in physiological environments rank it over other biomedical materials in terms of resorbability and in vivo replacement by new bone tissue [11,12]. Conventionally β-TCP can be synthesized via a solid-state process [3] or by thermal decomposition of amorphous calcium phosphate or calcium deficient apatite obtained by the wet chemical method [4,13]. Upon heat treatment at 700–800 °C the non-stoichiometric apatite (Ca deficient) is transformed into β-TCP [14,15] according to the following equation:

$$Ca_9(HPO_4)(PO_4)_5(OH) \rightarrow 3Ca_3(PO_4)_2 + H_2O \quad (1)$$

Attempts to get more insight into this transformation showed that the calcium phosphate ratio (Ca/P) of the non-stoichiometric reagent not only conditions the temperature of the transformation reaction but also the reaction product crystal phase composition as a biphasic mixture of HAP and β-TCP may also result. For some biomedical applications, the degradation behaviour of synthetic HAP might be too slow and a CaP material with a faster resorption could be necessary in order to accelerate the bone replacement process. For this reason composites made of β-TCP and HAP, the so called

* Corresponding author. Tel.: +351 234370254; fax: +351 234370204.
E-mail address: elisabete.costa@ua.pt (M.E.V. Costa).

0272-8842/$34.00
doi:10.1016/j.ceramint.2008.08.015

biphasic calcium phosphates (BCPs), which combine the excellent bioactivity of HAP with the good bioresorbability of β-TCP [16–18], are interesting candidates for bone replacement and drug delivery systems (DDS) [19,20].

The biological performance of CaP materials is also conditioned by their morphological characteristics being known that CaP granules with smooth spherical geometry are preferable as drug delivery systems and for restorative surgery in order to minimize inflammatory processes [21]. Among the reported methods for producing CaP granulates [21–25], the conventional spray drying technique stands up for obtaining nearly spherical and porous granules with uniform morphology. Besides favouring cell adhesion, granules having porous structure are well suited to be easily impregnated with solutions or suspensions of various drugs and then perform as drug carriers.

5-Fluorouracil (5FU) is an antineoplastic agent used in the therapy of different solid tumours [26]. Aiming at the ideal DDS which would release the 5FU drug to the desired site at an appropriate rate while ensuring minimum side effects at non-target sites, different polymeric carriers were already reported [27–33]. The possible synergies between 5FU effects and the biological properties of some calcium phosphates also led to different attempts relying on β-TCP or HAP as 5FU carriers [34,35]. In particular HAP granules loaded with 5FU may offer the anti-tumour effectiveness of 5FU with a certain reduction of the drug poisonous by-effects [35–37]. However in this case [35] the reported results revealed a too high release rate of 5FU which still requires optimization.

The objective of the present study is to develop an improved delivery system, based on two different types of calcium phosphate granules, for the local administration of 5-Fluorouracil. For this purpose calcium phosphate porous granules were prepared and characterized. Their adsorption and in vitro release kinetics of the anticancer drug 5-Fluorouracil were evaluated and correlated with the granules characteristics.

2. Materials and methods

2.1. Materials

The following chemicals were used without further purification: citric acid (Riedel-deHaën, 99.5%); Ca $(NO_3)_2{\cdot}4H_2O$ (Riedel-deHaën, 99%); $(NH_4)_2HPO_4$ (Merck 99%); ammonia solution, 25% (Riedel-deHaën); 5-Fluorouracil (sigma 99) (5FU). Porous HAP granules to be used as drug adsorbents were prepared by spray drying suspensions of hydroxyapatite (HAP) nanoparticles (∼1 wt.%) which in a first step were precipitated from calcium/citrate/phosphate solutions [1] as follows: a citrate–ammonium solution with a controlled pH (8.15) was prepared and to this solution were added, under stirring, $Ca(NO_3)_2{\cdot}4H_2O$ (0.2 M) and $(NH_4)_2HPO_4$ (0.2 M) solutions. The so obtained solution was then passed through a 0.45 μm Millipore filter and placed in a water bath at 37 °C, for a period of 24 h. The powders resulting from precipitation were separated by centrifugation in an ultracentrifuge (Beckman L8-70 M) at 10,000 rpm at 10 °C for 15 min. The supernatant liquid was discarded and the powder was washed in distilled water and dried in a desiccator.

The preparation of apatite particles by spray drying required the following steps: (i) apatite nanoparticles were suspended in distilled water (∼1 wt.%) and then (ii) used as the feeding flow of a laboratory spray dryer (Buchi B-191). Operating conditions of the spray dryer included an inlet temperature of 170 °C and a spray feed flow of 6 ml/min. The spray dried particles were collected from the cyclone.

The spray dried apatite granules (SDG) were heat treated at 800 °C during 2 h with a 10 °C/min heating rate. The SDG and the heat treated SDG (hereafter called HSDG) were tested as adsorbent and releasing system of the drug 5FU.

2.2. Powder characterization

The crystalline phases were identified by powder X-ray diffraction (XRD) analysis (Rigaku PMG-VH with CuKα radiation = 1.5405 Å). The calcium and phosphorus contents of the precipitated HAP nanoparticles were assayed by inductively coupled plasma spectroscopy (ICP) (ISA Jobin Yvon–JY70 Plus). The morphology and structure of SDG and HSDG were observed by scanning electron microscopy (SEM) (Hitachi S-4100) and transmission electron microscopy (TEM) (Hitachi H-9000-NA, 300 kV accelerating potential). For TEM analysis the powders were ground in a mortar, then dispersed with 2-propanol and scattered over copper grids covered with formvar film. Fourier transform infrared spectroscopy (FTIR) (Mattson galaxy 3020) in transmittance mode was used to identify the particles functional groups in the range of 400–4000 cm^{-1}, using KBr pellets. The specific surface area (SSA) of the granules was determined by N_2 gas adsorption, using the multipoint Brunauer–Emmett–Teller isotherm (BET) in a Micromeritics Gemini 2370 V5 equipment. Both differential thermal and thermogravimetric analyses (DTA and TGA) were conducted on SDG to follow their thermal behaviour. The analyses were performed from room temperature up to 1000 °C, with a 10 °C/min heating rate (Setaram Labsys 1600 under N_2 flow) and complemented by FTIR spectroscopy and XRD analysis of the SDG calcined at several temperatures (200, 600 and 800 °C).

2.3. Drug loading and delivering

Loading of both types of granules, the as-spray dried (SDG) and the heat treated at 800 °C (HSDG) with 5FU was performed via a soaking procedure in 100 ml of a 250 mg/L 5FU solution, at pH 5.2 and room temperature, for several days. The adsorbed amount of 5FU by the granules was evaluated by UV–vis spectroscopy, using the measured maximum absorbance of 5FU in solution at 265.5 nm [5]. The adsorbed amount of 5FU per unit weight of HAP granules (Q) was determined from the relation $Q = V(\Delta C)/W$, where V(L) is the volume of the soaking solution in contact with the mass of granules W(g), and ΔC the difference between the initial C_0 (g/L) and the final C_e (g/L) concentrations of 5FU in the soaking solutions. The time dependence of the adsorbate concentration in the soaking

solution was monitored. After soaking, the particles were filtered off, washed with deionized-distilled water and finally dried in a desiccator.

In vitro release of 5FU was assayed by immersing the loaded granules in phosphate buffered solution (PBS) with pH 7.4 at 37 °C. The measurement of the released amount of 5FU in solution was evaluated by UV–vis spectroscopy at 265.5 nm.

For comparing the behaviour of both 5FU loaded and unloaded HSDG in a phosphate buffer solution, some HSDG were immersed in PBS in the same conditions (time, temperature and pH).

3. Results and discussion

3.1. Characterization of the spray dried particles

The granules SDG produced by spray drying the suspension of apatite nanoparticles were characterized as hydroxyapatite (HAP) according to their X-ray diffraction pattern (Fig. 1a) and no other crystalline phase was detected. The calcium phosphate ratio (Ca/P) of both precipitated nanoparticles and SDG was 1.68. Although this value exceeds the stoichiometric Ca/P it is thought that the precipitated particles (and SDG) are calcium-deficient HAP being its apparent calcium surplus explained by the presence of an amorphous calcium phosphate phase in the precipitated particles and the existence of adsorbed calcium–citrate complexes, as reported before [38]. After calcining the granules at 800 °C significant modifications in crystalline phase composition were noticed. As shown in Fig. 1 a remarkable increase of HAP crystallinity together with the crystallization of one new phase, β-tricalcium phosphate (β-TCP), are observed at 800 °C. Following literature reports [14,39] the appearance of β-TCP may be explained as a HAP transformation reaction product according to Eq. (1).

Fig. 2 characterizes the thermal behaviour of the granules SDG in the temperature range $25 < T < 1000$ °C. As observed different weight losses occur at different temperature ranges: (i) an initial steep weight loss ($25 \leq T \leq 150$ °C) accompanied by an endothermic peak is assigned to the release of weakly

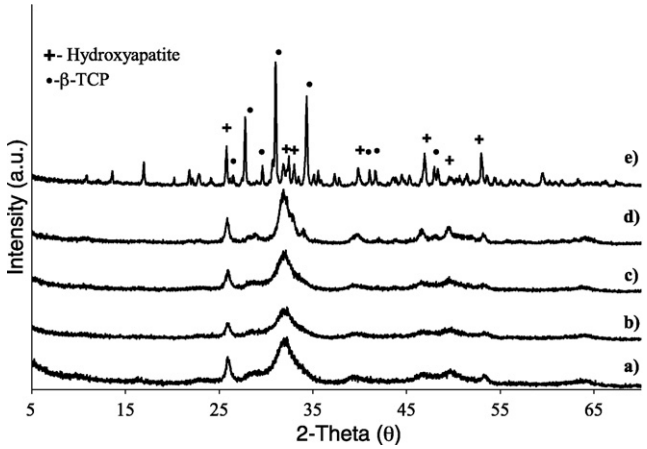

Fig. 1. XRD patterns of SDG (a), SDG heat treated at 200 °C (b), 400 °C (c), 600 °C (d) and 800 °C (e).

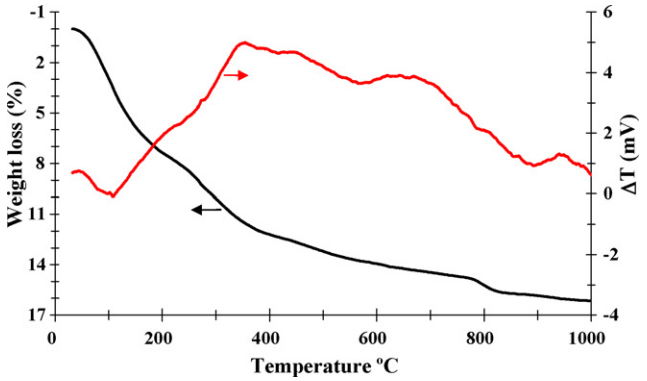

Fig. 2. Thermal analyses (DTA and TGA) of SDG.

physisorbed water; (ii) for temperature increasing beyond 150 °C distinct weight loss regimes followed by broad exothermic effects are also identified. As previously reported [38,40] citrate groups derived from the original precipitating medium of HAP nanoparticles exist as adsorbed species at the surface of the granules SDG but undergo exothermic decomposition reactions during heat treatment thereby giving place to weight losses and heat release. Furthermore a small but well defined weight loss around 800 °C is worthy being remarked as it can be attributed to the release of water accompanying the phase transition from HAP to β-TCP, as predicted by Eq. (1).

In line with XRD results, the FTIR spectra of the HSDG (Fig. 3) also evidence the formation of biphasic mixtures of HAP and β-TCP at 800 °C as confirmed by the decrease in a broad band corresponding to the vibration of the OH group at 3569 cm^{-1} [14]. Moreover other vibrational bands assigned to β-TCP are also present, although they are superimposed by others more intense groups. The evolution of SDG granules FTIR spectra with increasing temperature also denotes the gradual loss of citrate carboxyl groups as indicated by the decrease in the sharpness of the corresponding peaks in the region around 1421 and 1598 cm^{-1}. Furthermore, new bands corresponding to stretching of carbonate groups substituting OH^- in A-type sites and PO_4^{3-} in B-type sites of HAP structure are evidenced at 600 °C (see Fig. 3) suggesting that citrate decomposition may account for these carbonate groups. At 800 °C citrate groups are no longer detected but carbonate bands are still present though with a much weaker intensity. These features are consistent with the contribution of citrate group degradation to the weight loss depicted in Fig. 2, as discussed above.

The spray dried granules (SDG) were donut shaped with an average diameter of 5 μm, as illustrated by SEM micrographs (Fig. 4a). Their large specific area (150 m^2/g) is of the same order of magnitude as that of the individual HAP nanoparticles (170 m^2/g). This fact indicates that the granules SDG are built by soft agglomeration of the precursor HAP nanoparticles during the spray drying process, thereby maintaining a nanometric but also porous architecture. After heat treatment at 800 °C the granules loose their donut shape becoming more spherical, as shown in the micrographs of Fig. 4b. The

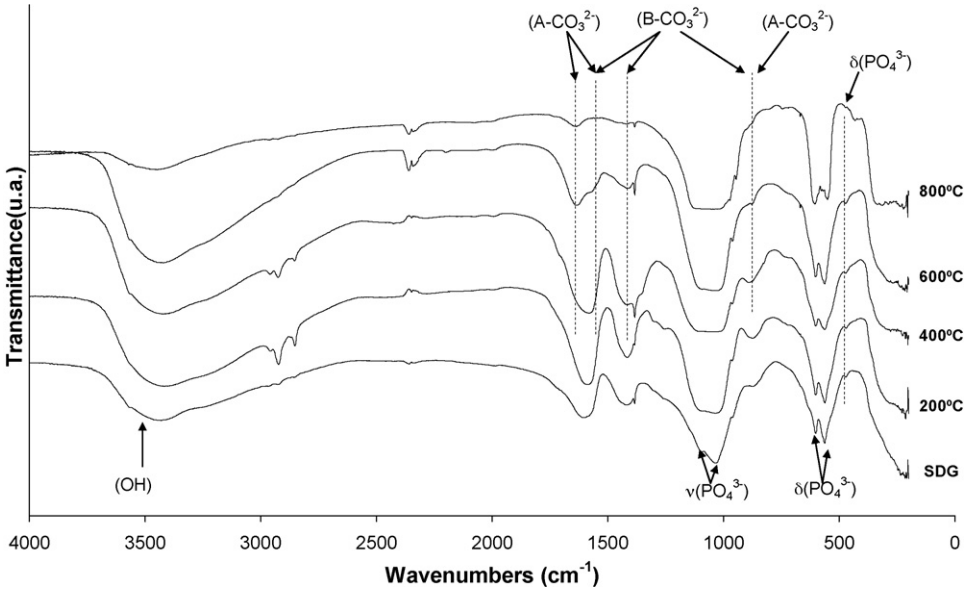

Fig. 3. FTIR spectra of SDG (a), SDG calcined at 200 °C (b), 400 °C (c), 600 °C (d) and 800 °C (e).

morphological changes accompanying the increase of temperature coincided with the strong variation of the specific surface area, which decreased from 150 m^2/g for the SDG to 6.2 m^2/g for HSDG.

3.2. Drug loading

Most of the studies concerning 5FU deal mainly with polymeric biodegradable supports such as chitosan [26,31], PLGA (poy(lactide-co-glycolide) [41] and PGLC (poy(lactide-co-glycolide-co-caprolactone). Reports on calcium phosphate carriers of 5FU are almost inexistent being β-TCP [34] a worthy mentioning example. In this last case the drug loading was ensured by a vacuum adsorption technique which seems more sophisticated than the loading technique used in the present work. The calcium phosphate granules here reported were simply soaked in a 5FU solution for several days which allowed the adsorption of 5FU on the surface of the granules.

Fig. 5 shows the time variation of the drug amount adsorbed by both type of adsorbents, i.e. the heat treated granules

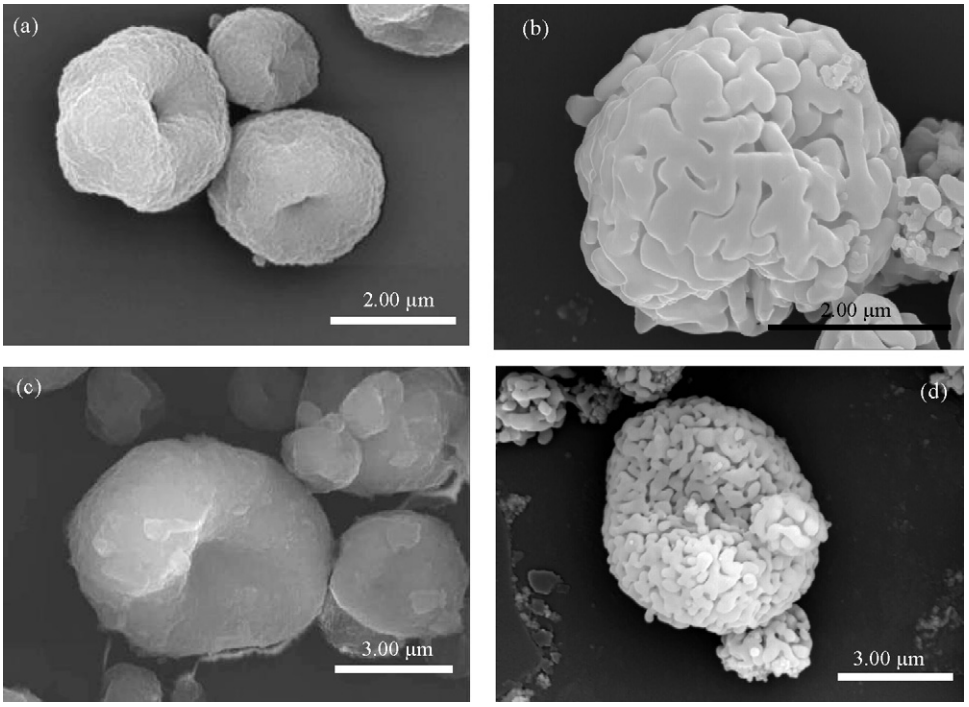

Fig. 4. Granules SEM images: spay dried granules (SDG) (a), granules heat treated at 800 °C (HSDG) (b), SDG after 5FU loading (c) and HSDG after 5FUloading (d).

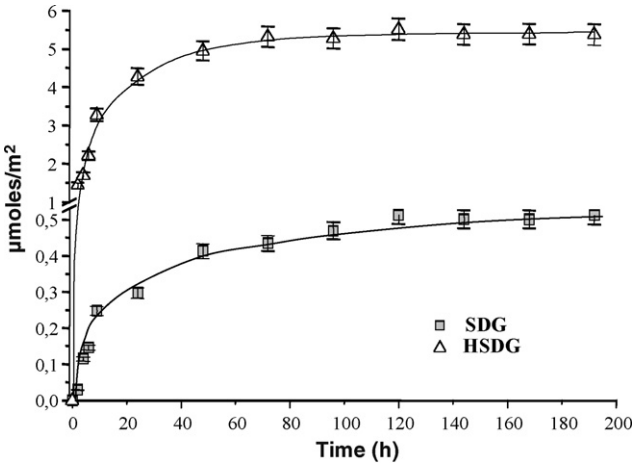

Fig. 5. Immersion time dependence of the 5FU adsorbed amount by SDG (-■–) and by HSDG (-△-).

(HSDG) and the untreated ones (SDG), when immersed into the 5FU solution having a concentration of 250 mg/L. As observed the initial fast increase of the adsorbed amount of 5FU gradually slows down towards a final plateau where a constant quantity of adsorbed drug is reached. The adsorption results obtained in the present work also demonstrate that the final amount of adsorbed drug per unit of surface area of HSDG (∼451 μg 5FU/m^2) was considerably larger than that corresponding to SDG (∼41 μg 5FU/m^2). This different adsorption behaviour may be assigned to the distinct morphological, compositional and surface state attributes of both types of granules. As discussed above, SDG and HSDG present different crystalline phase composition and different morphologies (Figs. 1 and 4) which were kept during the 5FU adsorption essay as accessed through the micrographs presented in Fig. 6. Furthermore, citrate groups were present in SDG but not in HSDG, as revealed by FTIR results (Fig. 3). Therefore these results point out to a different adsorptive ability of each type of granule relying on their surface chemical composition, mainly on the presence or absence of citrate groups. According to previous studies the presence of adsorbed citrate groups contributes to lower the granule zeta potential and by this way to decrease the adsorbing ability of the granules towards 5FU [40]. As heat treatment of the granules at 800 °C decomposed citrate groups, these chemical species could no longer interfere on HSDG particle surface charge establishment thereby explaining the increased adsorption ability of the heat treated granules towards 5FU [40]. Besides citrate groups, other factors might have also to be taken into account for explaining the adsorption behaviour differences between SDG and HSDG. Hydroxyapatite and β-TCP are crystallographically different: whereas HAP has a hexagonal structure, β-TCP is rhombohedral, and the surface planes of major density of calcium and phosphorus ions are different in both structures [9]. It can thus be expected that the two crystal phases will reveal different abilities for the adsorption of the 5FU molecule. Moreover, the

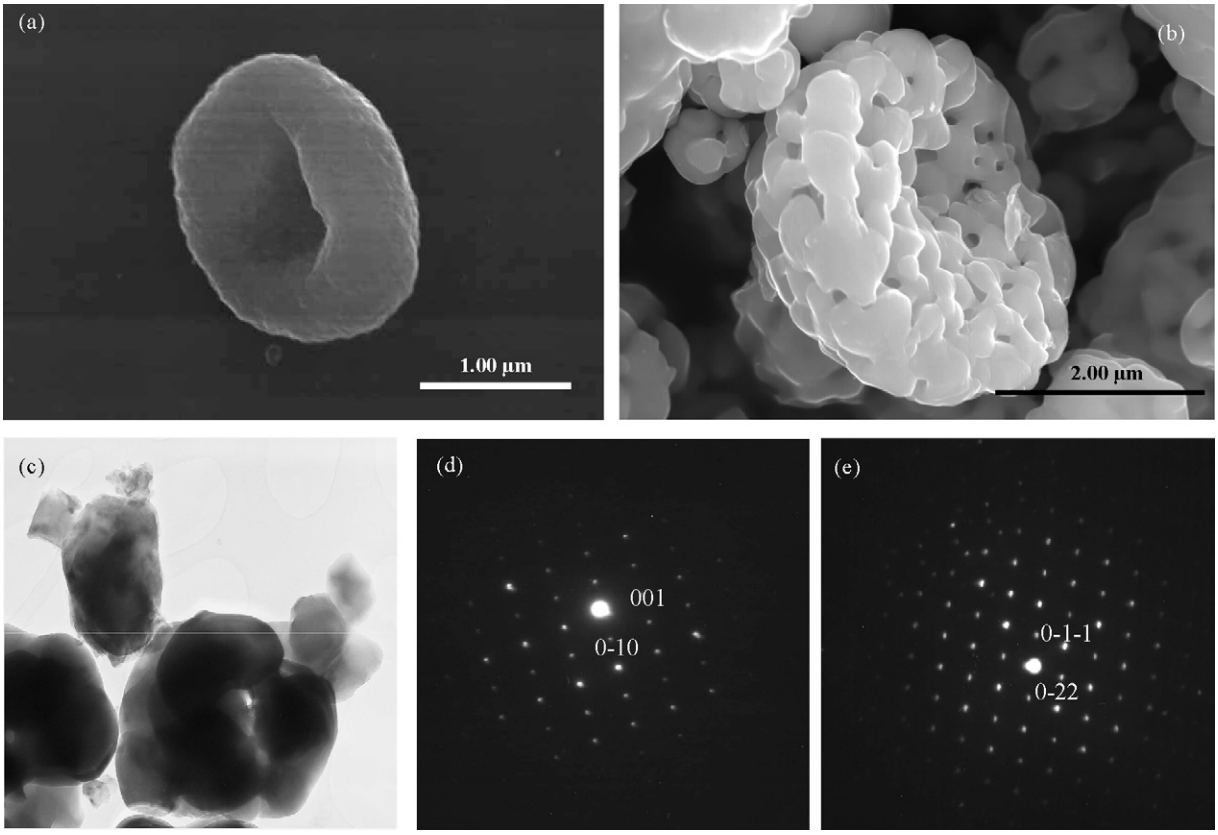

Fig. 6. SEM picture of SGD (a) and of HSGD (b) after 5FU release in a phosphate buffered solution; TEM microstructure of HSDG after 5FU release (c) showing the presence of HAP indicated by the selected diffraction pattern from its [100] zone axis (d) and of β-TCP indicated by the selected diffraction pattern from its [100] zone axis (e).

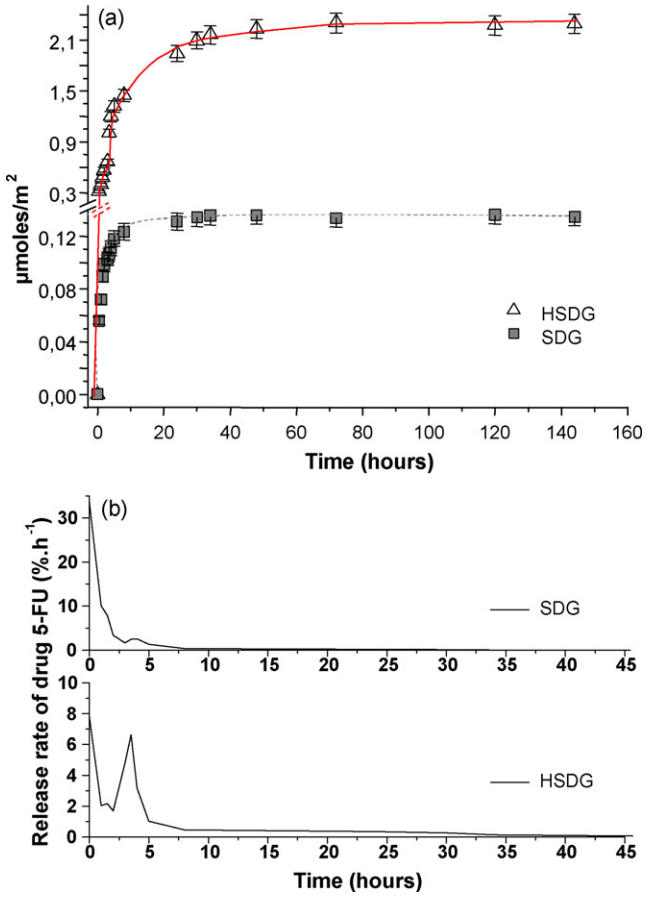

Fig. 7. Time dependence of the 5FU released amount for (-□-) SDG and (-△-) HSDG (a); time dependence of 5FU release rate for SDG and HSDG (b).

higher adsorption ability of the heat treated granules at 800 °C can also reflect the presence of a higher concentration of defects on their surface, which might offer additional active adsorption locations [9].

3.3. Drug delivery

Fig. 6 shows the SDG and HSDG SEM micrographs obtained after seven days of immersion in the PBS solution used for assessing the 5FU release. As observed for both type of granules any noticeable morphology modification is identified when comparing the pictures obtained before and after drug release (Figs. 4 and 6). This fact suggests that the granules integrity is preserved during the loading and delivering period. The release profiles of 5FU by SDG and HSDG in a phosphate buffer solution are displayed in Fig. 7a. For both type of granules the release of the drug was very fast at the beginning, decreasing then gradually after the initial time period. After two days (48 h) the drug release is complete in both delivery systems. This equilibrium time of two days exceeds largely the time of 5 min previously reported for HAP granules [35], being similar to that observed for other carrier materials [31,34,41] having equivalent amounts of loaded drug although shorter than the time required by β-TCP blocks loaded with higher amounts of 5FU [34].

Despite the similarity of equilibrium times, significant differences are noticed in the total amount of the released drug by the two types of granules here reported: for HSDG it reaches ~27.5% of the loaded drug (corresponding to 9 μmol/L) whereas for SDG it attains 40% of the loaded drug (corresponding to 30 μmol/L). Besides that the drug release rates from SDG and from HSDG are also distinct as concluded from Fig. 7b: while the release rate of 5FU from the untreated granules decreases with time almost gradually, the treated ones show a release maximum after ~3.5 h. These results point to different mechanisms ruling the 5FU release process from the two types of granules, probably accounted by their different surface characteristics which outcome from their different crystal phase composition and from their different contents of adsorbed citrate group, as referred before. According to the present data HSDG surface displays a higher ability to adsorb 5FU as compared to SDG but its releasing behaviour shows an opposite tendency since the drug amount released from SDG clearly exceeds that corresponding to HSDG. This might indicate a stronger bonding of 5FU to HSDG than to SDG surface.

XRD patterns of SDG and HSDG obtained before and after the drug release process are compared in Figs. 8 and 9. Besides the general decrease of the granules crystallinity an apparent modification of HSDG crystal phase composition during the drug release period is also observed as β-TCP is the only detected phase after 5FU release. The absence of HAP in the (former) biphasic granules may suggest that Hydroxyapatite is the crystal phase degrading preferentially in the present system. As β-TCP has been often reported to degrade faster as compared to HAP [42], HSDG were further analysed in order to clarify whether or not HAP is present in the HSDG after the drug release. Electron diffraction (ED) results (TEM) respecting HSDG after drug release where examined and the indexing of selected area diffraction patterns presented in Fig. 6 enabled two different crystal structures corresponding to HAP and to β-TCP to be identified. It is concluded that HAP crystalline phase is still present in HSDG after the drug release experiment but

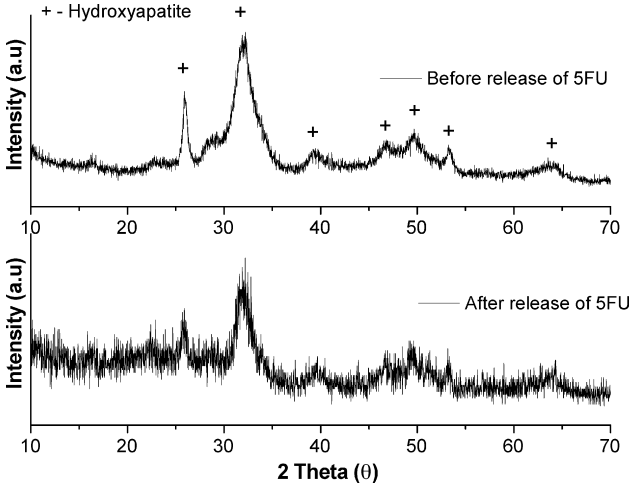

Fig. 8. XRD patterns of SGD before 5FU release (a) and after 5FU release (b).

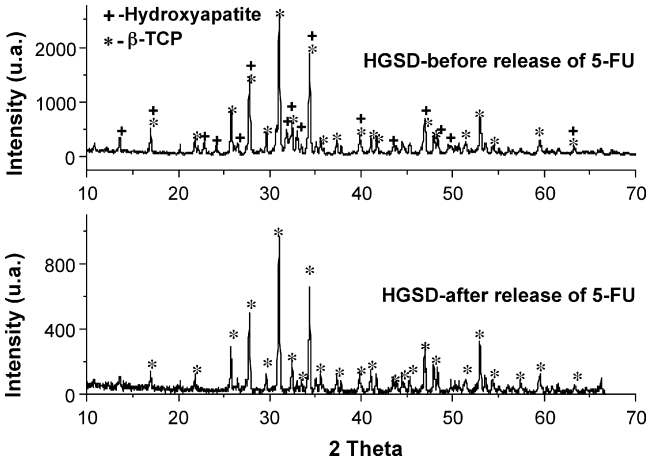

Fig. 9. XRD patterns of HSDG before 5FU release (a) and after 5FU release (b).

probably in amounts too small to be detected by X-ray analysis.

The observed crystal modifications and their interplay with the 5FU release process itself are now under investigation.

For demanding biomedical applications requiring the combination of a drug delivery system with a scaffold material for bone tissue engineering. heat treated granules may offer certain advantages. The present results foresee that β-TCP present on HSDG might be the crystal phase that under circumstances comparable to those reported in this paper remains longer and whose presence is desirable as it can contribute to a faster bone tissue formation, due to its greater osteoconductivity in vivo [43].

4. Conclusion

Porous apatite granules produced by spray drying suspensions of hydroxyapatite nanoparticles were heat treated at 800 °C for 2 h. The calcination modified the morphology of the granules and promoted the transformation of a poorly crystalline HAP into a biphasic mixture of a more crystalline HAP and a crystalline β-TCP. In addition the surface reactivity of the granules through the elimination of the adsorbed citrate species, resulting from the HAP nanoparticles synthesis process, was also modified. Consequently a significant increase of the adsorptive capacity of the granules towards the drug 5-Fluorouracil occurred. Furthermore the drug release rates were different being even noticed an opposite trend in the drug releasing ability of the granules as confirmed by the larger amount of released 5FU by the untreated granules as compared to the heat treated ones. Since the particular drug release profile exhibited by each type of granule was accompanied by a variation of its crystallinity a possible interplay between the 5FU release process and the dynamics of the granule crystal phase evolution are here addressed.

Acknowledgment

This work was supported in part by the European Project G5RD-CT2000-00282 Tissue Reactor.

References

[1] M.A. Martins, C. Santos, M.E.V. Costa, M.M. Almeida, Preparation of porous hydroxyapatite particles to be used as drug delivery systems, Advanced Materials Forum II (455) (2004) 353–357.
[2] R.-P. Franke, C. Santos, T. Scharnweber, M.M. Almeida, M.E.V. Costa, Influence of nanostructured calcium-phosphate particles on rat osteosarcoma cells, Basic and Clinical Pharmacology and Toxicology 101 (5) (2007) 360–1360.
[3] A. Cüneyt Tas, F. Korkusuz, M. Timuçin, N. Akkas, An investigation of the chemical synthesis and high-temperature sintering behaviour of calcium hydroxyapatite (HA) and tricalcium phosphate (TCP) bioceramics, Journal of Materials Science: Materials in Medicine 8 (1997) 91–96.
[4] Jong-Shing Bow, Sz-chian Liou, San-Yuan Chen, Structural characterization of room-temperature synthesized nano-sized β-tricalcium phosphate, Biomaterials 25 (2004) 3155–3161.
[5] F.N. Oktar, Microstructure and mechanical properties of sintered enamel hydroxyapatite, Ceramics International 33 (7) (2007) 1309–1314.
[6] Milenko Markovic, Bruce O. Fowler, Ming S. Tung, Preparation and comprehensive characterization of a calcium hydroxyapatite reference material, Journal of Research of the National Institute of Standards and Technology 109 (6) (2004) 553–568.
[7] YingJun Wang, Shuhua Zhang, Kun Wei, Naru Zhao, Jingdi Chen, Xudong Wang, Hydrothermal synthesis of hydroxyapatite nanopowders using cationic surfactant as templates, Materials Letters 60 (2006) 1484–1487.
[8] T.L. Livingston, S. Gordon, M. Archambault, S. Kadiyala, K. Mcintosh, A. Smith, S.J. Peter, Mesenchymal stem cells combined with biphasic calcium phosphate ceramics promote bone regeneration, Journal of Materials Science: Materials in Medicine 14 (2003) 211–218.
[9] J.C. Elliott, Structure and Chemistry of the Apatites and Other Calcium Orthophosphates, vol. 18, Elsevier, 1994, pp. 111–116.
[10] Xilin Yin, M.J. Stott, α and β-tricalcium phosphate: a density functional study, Physical Review B 68 (205) (2003) 1–8.
[11] Kaili Lin, Jiang Chang, Jianxi Lu, Wei Wu, Yi Zeng, Properties of β-$Ca_3(PO_4)_2$ bioceramics prepared using a nano size powders, Ceramics International 33 (6) (2007) 979–985.
[12] Hisaya Orii, Shinichi Sotome, Jiani Chen, Juyong Wang, Kenichi Shinomiya, β tricalcium phosphate (β-TCP) graft combined with bone marrow stromal cell (MSCs) for posterolateral spine fusion, Journal of Medical Dental Science 52 (2005) 51–57.
[13] K.S. Jaw, Preparation of a biphasic calcium phosphate from $Ca(H_2PO_4)_2{\cdot}H_2O$ and $CaCO_3$, Journal of Thermal Analysis and Calorimetry 83 (1) (2006) 145–149.
[14] I.R. Gibson, I. Rehman, S.M. Best, W. Bonfield, Characterization of the transformation from calcium-deficient apatite to β-tricalcium phosphate, Journal of Materials Science: Materials in Medicine 11 (12) (2000) 799–804.
[15] N. Koc, M. Timucin, F. Korkusuz, Fabrication and characterization of porous tricalcium phosphate ceramics, Ceramics International 30 (2) (2004) 205–211.
[16] N. Rangavittal, A.R. Landa-Cánovas, J.M. Gonzalez-Calbet, M. Vallet-Regi, Structural study and stability of hydroxyapatite and α-tricalcium phosphate: two important bioceramics, Journal Biomedical Materials Research 51 (4) (2000) 660–668.
[17] Li-Chun Lin, Shwu-Jen Chang, Shyh Ming Kuo, Shu Fen Chen, Chia Hung Kuo, Evaluation of chitosan/β-tricalcium phosphate microspheres as a constituent to PMMA cement, Journal of Materials Science: Materials in Medicine 16 (2005) 567–574.
[18] C. Santos, R.-P. Franke, M.M. Almeida, M.E.V. Costa, M.H. Fernandes, Behaviour of Osteoblastic-Like MG-63 Cells Cultured with Hydroxyapatite and Biphasic (Hap/β-TCP) porous granules, Tissue Engineering-Part A 14 (5) (2008) 810–1810.
[19] Hae-Won Kim, Jonathan C. Knowles, Hyoun-Ee Kim, Hydroxyapatite/poly(e-caprolactone) composite coating on hydroxyapatite porous bone scaffolds for drug delivery, Biomaterials 25 (2004) 1279–1287.
[20] Y.H. Hsu, I.G. Turner, A.W. Miles, Fabrication and mechanical testing of porous calcium phosphate bioceramic granules, Journal of Materials Science: Materials in Medicine 18 (10) (2007) 1931–1937.

[21] V.S. Komlev, S.M. Barinov, E. Girardin, S. Oscarsson, A. Rosengren, F. Rustichelli, V.P. Orlovskii, Porous spherical hydroxyapatite and fluorhydroxyapatite granules: processing and characterization, Science and Technology of Advanced Materials 4 (2003) 503–508.
[22] P. Luo, T.G. Nieh, Synthesis of ultrafine hydroxyapatite particles by a spray dry method, Materials Science and Engineering C3 (1995) 75–78.
[23] P. Luo, T.G. Nieh, Preparing hydroxyapatite powders with controlled morphology, Biomaterials 17 (1996) 1959–1964.
[24] C.C. Ribeiro, C.C. Barrias, M.A. Barbosa, Calcium phosphate-alginate microspheres as enzyme delivery matrices, Biomaterials 25 (2004) 4363–4373.
[25] Willi Paul, Chandra P. Sharma, Infection resistant hydroxyapatite/alginate plastic composite, Journal of Materials Science Letters 16 (1997) 2050–2051.
[26] Y. Zheng, W. Yang, C. Wang, J. Hu, S. Fu, L. Dong, L. Wu, X. Shen, Nanoparticles based on the complex of chitosan and polyaspartic acid solution salt: preparation, characterization and the use for 5-fluorouracil delivery, European Journal of Pharmaceutics and Biopharmaceutics 67 (2007) 621–631.
[27] Alf Lamprecht, Hiromitsu Yamamoto, Hirofumi Takeuchi, Yoshiaki Kawashima, Microsphere design for the colonic delivery of 5-fluorouracil, Journal of Controlled Release 90 (2003) 313–322.
[28] Anshul Gupte, Kadriye Ciftci, Formulation and characterization of paclitaxel, 5-FU and Paclitaxel+5-FU microspheres, International Journal of Pharmaceutics 276 (2004) 93–106.
[29] B. Arica, S. Çalis, H.S. Kas, M.F. Sargon, A.A. Hincal, 5-Flourouracil encapsulated alginate beads for the treatment of breast cancer, International Journal of Pharmaceutics 242 (2002) 267–269.
[30] D. Bhadra, S. Bhadra, S. Jain, N.K. Jain, A PEGylated dendritic nanoparticulate carrier of fluorouracil, International Journal of Pharmaceutics 257 (2003) 111–124.
[31] E.B. Denkbas, M. Seyyal, E. Piskin, Implantable 5-fluorouracil loaded chitosan scaffolds prepared by wet spinning, Journal of Membrane Science 172 (2000) 33–38.
[32] E. Fournier, C. Passirani, A. Vonarbourg, L. Lemaire, N. Colin, S. Sagodira, P. Menei, J.-P. Benoit, Therapeutic efficacy study of novel 5-FU-loaded PMM 2. 1. 2-based microspheres on C6 glioma, International Journal of Pharmaceutics 268 (2003) 31–35.
[33] Feng Qian, Norased Nasongkla, Jinming Gao, Membrane-encased polymer milirods for sustained release of 5-flourouracil, Journal of Biomedical Materials Research 61 (2002) 203–211.
[34] E. Landi, L. Orlandi, G. Spagna, A. Tampieri, N. Zaffaroni, Calcium phosphate ceramics as drug-delivery system for anticancer therapy, Key Engineering Materials 192–195 (2001) 901–904.
[35] C. Santos, C.F. Rovath, R.-P. Franke, M.M. Almeida, M.E.V. Costa, Spray-dried hydroxyapatite-5-Fluorouracil granules as a chemotherapeutic delivery system, Ceram. Int. 35 (2009) 509–513.
[36] Xiaojuan Chen, Changsheng Deng, Shangli Tang, Ming Zhang, Mitochondria-dependent apoptosis induced by nanoscale hydroxyapatite in human gastric cancer SGC-7901 cells, Biological Pharmaceutics Bulletin 30 (1) (2007) 128–132.
[37] Jun Hu, Zhi-Su Liu, Shangli Tang, Yue-Ming He, Effect of hydroxyapatite nanoparticles on the growth and p53/c-Myc protein expression of implanted hepatic VX2 tumor in rabbits by intravenous injection, World Journal Gastroenterology 13 (20) (2007) 2798–2802.
[38] M.A. Martins, C. Santos, M.M. Almeida, M.E.V. Costa, Hydroxyapatite micro- and nanoparticles: nucleation and growth mechanisms in the presence of citrate species, Journal of Colloid and Interface Science 318 (2) (2007) 210–216.
[39] Giuliano Gregori, Hans-Joachim Kleebe, Helmar Mayr, Gönter Ziegler, EELS characterization of β-tricalcium phosphate and hydroxyapatite, Journal of the European Ceramic Society 26 (2006) 1473–1479.
[40] C. Santos, M.A. Martins, M.M. Almeida, M.E.V. Costa, Adsorption mechanism of 5-Flourouracil on different hydroxyapatite particles, Advanced Materials Forum III (514) (2006) 1103–1110.
[41] X. Li, Y. Xu, G. Chen, P. Wei, Q. Ping, PLGA nanoparticles for the oral delivery of 5-Fluorouracil using high pressure homogenization-emulsification as the preparation method and in vitro/in vivo studies, Drug Development and Industrial Pharmacy 34 (2008) 107–115.
[42] G. Daculsi, Biphasic calcium phosphate concept applied to artificial bone, implant coating and injectable bone substitute, Biomaterials 19 (1998) 1473–1478.
[43] Angela M.H. Ng, K.K. Tan, M.Y. Phang, O. Aziyati, G.H. Tan, M.R. Isa, B.S. Aminuddin, M. Naseem, O. Fauziah, B.H.I. Ruszymah, Journal of Biomedical Materials Research Part A 85A (2) (2008) 301–312.